JACS
JOURNAL OF THE AMERICAN CHEMICAL SOCIETY
Cite This: J. Am. Chem. Soc. 2018, 140, 6441−6447
Article
pubs.acs.org/JACS

Potent Macromolecule-Sized Poration of Lipid Bilayers by the Macrolittins, A Synthetically Evolved Family of Pore-Forming Peptides

Sijia Li,[†] Sarah Y. Kim,[†] Anna E. Pittman,[§] Gavin M. King,[§,∥] William C. Wimley,*[,‡] and Kalina Hristova*[,†]

[†]Materials Science and Engineering, Johns Hopkins University, Baltimore, Maryland 21218, United States
[‡]Biochemistry and Molecular Biology, Tulane University School of Medicine, New Orleans, Louisiana 70112, United States
[§]Physics and Astronomy, University of Missouri, Columbia, Missouri 65201, United States
[∥]Biochemistry, University of Missouri, Columbia, Missouri 65201, United States

ABSTRACT: Pore-forming peptides with novel functions have potential utility in many biotechnological applications. However, the sequence−structure−function relationships of pore forming peptides are not understood well enough to empower rational design. Therefore, in this work, we used synthetic molecular evolution to identify a novel family of peptides that are highly potent and cause macromolecular poration in synthetic lipid vesicles at low peptide concentration and at neutral pH. These unique 26-residue peptides, which we call macrolittins, release macromolecules from lipid bilayer vesicles made from zwitterionic PC lipids at peptide to lipid ratios as low as 1:1000, a property that is almost unprecedented among known membrane permeabilizing peptides. The macrolittins exist as membrane-spanning α-helices. They cause dramatic bilayer thinning and form large pores in planar supported bilayers. The high potency of these peptides is likely due to their ability to stabilize bilayer edges by a process that requires specific electrostatic interactions between peptides.

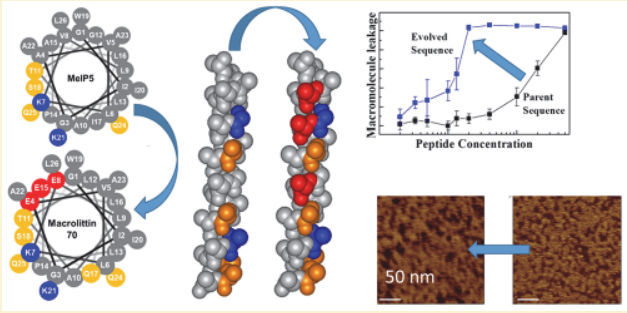

INTRODUCTION

Several thousand peptides that interact with and permeabilize lipid bilayer membranes have been described in the literature.[1] Peptides of this class have many potential uses in biotechnology, including use as antibacterial agents,[2] anticancer agents,[3] antiviral agents,[4] drug delivery vehicles,[5] transfection reagents,[6] exogenous ion channels,[7] and more. Successful applications have been limited, however, by several impediments. For example, some membrane permeabilizing peptides are active only at high concentration. Also, most pore forming peptides form small, transient pores in bilayers.[8−10] Despite very active research over the past few decades, our understanding of the sequence−structure−function relationships for membrane active peptides remains mostly descriptive, and not predictive. Thus, the current state of understanding does not readily enable rational design or improvement of membrane permeabilizing peptide activity.

In the absence of reliable predictive rules and algorithms for engineering the activity of membrane permeabilizing peptides, we have been using synthetic molecular evolution, i.e., iterative combinatorial library design and high-throughput screening, to discover new functionalities.[11−18] We began this effort with a first generation in which we screened a library based on the cytolytic bee venom peptide melittin, which forms transient pores,[9,10] for gain-of-function analogs that form equilibrium pores at much lower concentration than melittin. We later showed that the best of the selected gain-of-function variants, called MelP5, readily released a 10 kDa dextran and other macromolecules from lipid vesicles at low concentration.[19] We then used MelP5 as a template for a second generation screen in which we selected for release of a 40 kDa dextran[11] at low concentration in a manner that is triggered only at pH < 5.5. Because MelP5 causes macromolecular poration in a pH-insensitive manner, the library from which these "pHD peptides" were selected included six protonatable aspartate or glutamate residues, among other variations, in a MelP5 template. The selected pHD peptides are inactive at pH 7, but are triggered by low pH to cooperatively bind to membranes, fold into amphipathic α-helices and induce membrane destabilization that enables the release of macromolecules at least as large as 40 kDa dextrans.[11] The pH values for 50% leakage are ∼5.5, and the pHD peptides cause macromolecular poration at peptide-to-lipid ratios (P:L) lower than 1:500.[19] The pHD peptides were more potent than MelP5 at pH 5, suggesting that MelP5 could be further optimized as a macromolecular pore-former.

Received: March 19, 2018
Published: April 25, 2018

DOI: 10.1021/jacs.8b03026
J. Am. Chem. Soc. 2018, 140, 6441−6447

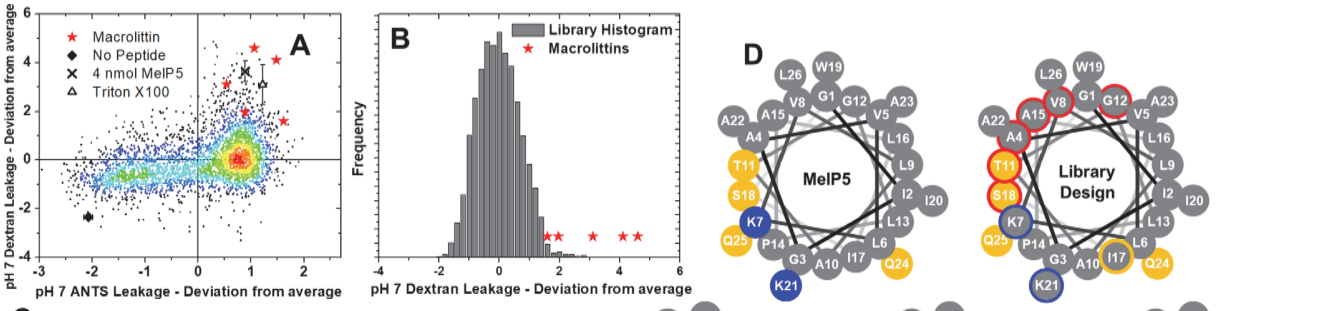

C

MelP5	GIGAVLKVLATGLPALISWIKAAQQL
Substitutions	L HD AL L QD H D E DD D E E EE E
Macrolittin70	GIGEVLKELATLLPELQSWIKAAQQL
Macrolittin159	GIGEVLHELATLLPELISWIKAAQQL
Macrolittin204	GIGDVLKELADLLPALQSWIKAAQQL
Macrolittin198	GIGDVLKDLADLLPLLQSWIKAAQQL
Macrolittin206	GIGEVLKVLAEELPLLQSWIKAAQQL
pHD15	GIGEVLHELADDLPDLQEWIHAAQQL
pHD24	GIGDVLHELAADLPELQEWIHAAQQL
pHD34	GIGEVLKELAADLPELQDWIKAAQQL
pHD54	GIGDVLKELADELPALQEWIHAAQQL
pHD63	GIGEVLKDLAAELPELQEWIHAAQQL
pHD101	GIGEVLKELADELPELQEWIHAAQQL
pHD108	GIGEVLHELAEGLPELQEWIHAAQQL
pHD118	GIGEVLHELADDLPELQSWIKAAQQL
pHD145	GIGDVLKELAEELPLLQEWIKAAQQL
pHD187	GIGEVLKDLADLLPELQEWIHAAQQL

Figure 1. Selection of macrolittins by synthetic molecular evolution. A. The results of the screen. *Z*-values (library member − plate mean)/ (plate standard deviation) for each library member are shown for the small molecule screen at pH 7 and for the macromolecule screen at pH 7. The macrolittins, red stars, were selected for simultaneous potent pore-forming activity in both screens. B. Histogram of macromolecule leakage values for the library members screened at P:L = 1:400 and pH 7. The macrolittins are in the most active 2% of the peptides screened. C. Table of peptide sequences. The sequence of the parent MelP5 and the MelP5-derived library is shown. The macrolittin sequences and pHD peptide sequences selected during the screens are also shown. Bold residues were varied. Acidic residues are red, basic residues are blue, hydrophobic residues are green, and polar residues are orange. D. Helical Wheel projections of the peptides discussed in this work. Acidic (red), basic (blue), and polar (yellow) residues are shown to highlight amphipathicity. Varied residues in the library are indicated by colored outlines, where red signifies acidic residues were included and blue signifies lysine and histidine were possible.

In this work, we sought to increase the diversity of well characterized peptides which can induce macromolecular poration. Specifically, we sought to identify new gain-of-function peptides that form macromolecule-sized pores in zwitterionic phosphatidylcholine bilayers with the same high potency as the pHD peptides, but which are active at neutral pH. To accomplish this, we used the MelP5-derived library from which the pHD peptides were selected, and performed a different high-throughput screen to select for peptides with the desired properties. As a result of this screen, we identified the "macrolittins", a novel family of peptides that induce macromolecular poration at neutral pH at remarkably low peptide to lipid ratios.

MATERIALS AND METHODS

Peptides and Lipids. The peptide library was synthesized by a split and recombine method and validated as described previously.[11,13−15] Single peptides were synthesized and purified by Biosynthesis Inc., and were verified by HPLC and mass spec. Lipids were purchased from Avanti Polar Lipids. TAMRA-biotin-dextran (TBD) was synthesized and purified as described previously.[11]

Vesicle Preparation. Two types of large unilamellar vesicles (LUV) containing different dyes (ANTS/DPX and TAMRA-biotin-dextran) were prepared. POPC lipids in chloroform were dried and then resuspended in a buffer with ANTS/DPX or TAMRA-biotin-dextran. The vesicles were frozen and thawed 10 times and then extruded through 0.1 μm Nucleopore polycarbonate filters 10 times to achieve a unilamellar uniform size. Vesicles with entrapped ANTS/DPX were separated from unentrapped ANTS/DPX by gel filtration chromatography. Unentrapped TBD was removed with streptavidin agarose. Lipid concentration was measured by Stewart Assay.[20]

Design of the Peptide Library. Previously, we described the design of the library from which we selected pH-sensitive macromolecular pore formers.[11] In short, we used the sequence of MelP5[19] as a template, and allowed six positions to be either the native residue, protonatable aspartate or glutamate, or sometimes an additional nonpolar residue. Positions 7 and 12, which are lysine in MelP5, were allowed to be either lysine or histidine. The isoleucine at position 17 was also allowed to be glutamine. The possible acidic residues were arranged to lie on one face of the amphipathic helix.

High-Throughput Screen. The library was synthesized as a one bead one sequence library and was screened using a serial, two-assay orthogonal screen. First, ~0.5 nmol of each library member in solution was assayed for induction of leakage of the small molecules ANTS and DPX[21] from POPC vesicles at pH 7 and a peptide to lipid ratio (P:L) = 1:200. Second, additional TBD vesicles were added at 30 min to screen for TAMRA-biotin-dextran (40 kDa) leakage at pH 7. The total P:L after the second addition was 1:400. For controls we also tested 4 nmol of MelP5 (final P:L = 1:50) for near complete macromolecule leakage. We also tested no peptide for a negative control and Triton-X100 detergent for a positive control for complete leakage. After

DOI: 10.1021/jacs.8b03026
J. Am. Chem. Soc. 2018, 140, 6441−6447

selection of the positive pore forming library members (see text) the peptide remaining on the bead was sequenced by Edman degradation.

Tryptophan Fluorescence. A Fluorolog3−22 spectrofluorometer with double-grating excitation and emission monochromaters was used to measure fluorescence spectra. The emission polarizer was oriented 0 degree relative to the vertical and the excitation polarizer at 90°. An excitation wavelength of 280 nm was used. Emission spectra were collected in the range of 300 to 450 nm for each sample.

Circular Dichroism (CD). CD spectra of MelP5 and macrolittins were measured in pH 7 phosphate buffer and in pH 5 acetate buffer, with and without 1 mM POPC vesicles. All CD spectra were recorded on a JASCO J715 CD spectrometer. Wavelength scans from 280 to 190 nm were performed in a 0.1 cm path length quartz cuvette using a slit width of 1 nm and a scan rate of 20 nm/min.

Oriented Circular Dichroism. Mixtures of peptide and lipid at P:L = 1:200 were prepared in methanol. Aliquots were dried onto a quartz disk which was sealed in a chamber with a second quartz window. The samples were hydrated through the vapor phase using a drop of distilled water in the chamber to form stacked oriented multibilayers. The quartz disk was oriented perpendicular to the beam and CD spectra were collected at eight rotations of the sample holder around the beam axis and averaged. Lipid-only spectra collected the same way were subtracted.

Sample Preparation for Atomic Force Microscopy (AFM) Imaging. We adopted established methods to form supported lipid bilayers on mica surfaces.[22] Briefly, POPC was suspended in 150 mM NaCl, 40 mM $CaCl_2$, and 20 mM HEPES, pH 5, at a concentration of 310 μM. Liposomes were prepared by extrusion of POPC through a polycarbonate membrane (approximately 25 times) with a 100 nm pore diameter. The peptide was diluted to a final concentration of 5 μM in imaging buffer: 100 mM NaCl, 50 mM HEPES at pH 5. POPC liposomes were incubated for 15 min in solution with the peptide to yield a final peptide concentration of 2.5 μM. The liposomes containing peptides were then deposited onto freshly cleaved mica. Supported bilayers were formed by vesicle fusion (30 min incubation, ~30 °C). Samples were rinsed four times using 75 μL of the imaging buffer. All data were collected at ~32 °C, which is significantly above the gel-to-fluid transition temperature of POPC.

AFM Imaging and Analysis. Images were acquired in tapping mode in aqueous buffer solution using a commercial apparatus (Asylum Research Inc., Cypher) and Biolever mini tips with spring constant $k \approx 0.9$ N/m (Olympus, BL-AC40TS). Care was taken to control the magnitude of the tip−sample force to ≤100 pN (estimated by comparing the free amplitude to the set point amplitude). As is typical, images were flattened (second order) to minimize background. For statistical analysis, the data were offset so as to align the population having the greatest height, corresponding to the top surface in each image, to zero. Defects were identified using a flood mask set at −0.3 nm with respect to this top surface.

RESULTS

Macromolecule Leakage Screen. The library design, shown in Figure 1C, uses MelP5 as a template and includes six sites in which protonatable aspartate or glutamate residues, as well as the original residue, were possible. In the screen, modified from one described previously,[11] two assays were performed in series. First, leakage of the small molecule fluorophore ANTS and its quencher DPX was measured at pH 7 and at P:L of 1:200. Next, additional vesicles containing entrapped TAMRA-biotin-dextran 40 kDa (TBD) and external AlexaFluor488-steptavidin were added to bring P:L to 1:400, a relatively low P:L value. Leakage of TBD was measured by assessing FRET between TBD and the labeled streptavidin after 1 h of incubation.

We screened 3200 library members, and the distribution of Z-values (standard deviations from individual plate averages) for the two assays are shown in Figure 1A. Controls included no peptide, Triton-X100 detergent for 100% release, and 4 nmol MelP5 which causes near total macromolecule release. For comparison, there was about 0.5 nmol of each library member present in the screen. The MelP5 controls correspond to P:L of 1:25 in the small molecule screen and P:L of 1:50 in the macromolecule screen. This amount of MelP5 releases nearly 100% of the small molecules ANTS and DPX and the dextran.

The majority of library members screened cause significant small molecule leakage, and moderate macromolecule leakage. Here, we are interested in the outliers that cause macromolecule release essentially equal to the positive controls. Therefore, positive peptides were selected from the area around the upper right-hand quadrant of the plot. This quadrant represents simultaneous very high small molecule leakage at pH 7 and very high macromolecule leakage at pH 7. Note that the leakage of the positives are all similar to the complete leakage caused by the detergent Triton X-100. The sequenced library members are shown as red stars. They are found in the upper 2 percentile of the screened sequences on the macromolecular leakage axis (Figure 1B). Thus, these peptides are gain-of-function daughter sequences of MelP5; they form macromolecule size pores in PC bilayers at pH 7 and at low peptide concentration. The screen suggested that the selected positives are much more potent than the parent peptide MelP5 at macromolecular poration, because ~0.5 nmol of these library members (P:L = 1:400) causes as much leakage as 4 nmol MelP5 control (P:L 1:50).

Sequence Analysis. The sequences of five selected peptides, which we named "macrolittins" are shown in Figure 1C along with the sequences of MelP5, the MelP5-based library, and the pHD peptides, for comparison. In Figure 1D we show helical wheel representations of the idealized helical surfaces of the parent MelP5, and representative members of the two peptide families. The macrolittins have a sequence motif that always contains three acidic residues, either glutamic or aspartic acid out of six possible acidic residues in the library. The probability of this occurring by chance five times (p) is 0.013. The acidic residues at the fourth and eighth positions are highly conserved (9/10 in total) in the five macrolittins. They are also conserved in the ten pHD peptides (20/20 total). The macrolittins sometimes have acidic residues in position 11 (3/5 peptides) and position 15 (2/5), but infrequently in position 12 (1/5) and position 18 (0/5), averaging about 1.0 acidic residues per peptide in those four positions. In comparison, each pHD peptide has either 3 or 4 acidic residues in those four positions, averaging 3.2 acidic residues per sequence in those four positions. More specifically, while positions 12 and 18 are acidic in the pHD peptides in 17 out of 20 chances, they are rarely acidic in the macrolittins (1/10) giving a probability of <0.0001 for this to have arisen by chance.

For the basic residues in positions 7 and 21 of the macrolittins, lysine was selected over histidine, 9 times in 10 chances (p = 0.01). This demonstrates a strong preference for lysine in the macrolittins that does not exist in the pHD peptides. Indeed, about half (11/20) of the possible basic residues in the pHD peptides were histidine instead of lysine. We note that both histidine and lysine are charged at pH < 5.5 where the pHD peptides are active, while only lysine is charged at pH 7 where the macrolittins are active.

Macromolecule Leakage. To fully characterize the sequences identified in the screen, we synthesized three representative macrolittins, 70, 159, and 204 (Figure 1) and measured their ability to permeabilize lipid vesicles made from

DOI: 10.1021/jacs.8b03026
J. Am. Chem. Soc. 2018, 140, 6441−6447

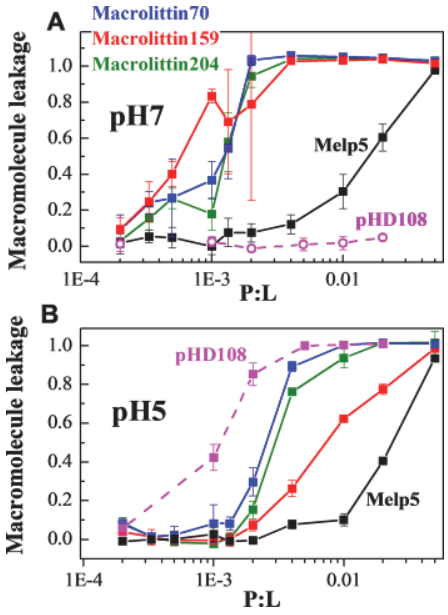

Figure 2. Macrolittin-induced leakage of a 40 kDa dextran from POPC vesicles. Vesicles with entrapped TAMRA-biotin-dextran 40 kDa (TBD) were incubated with serial dilutions of peptide in the presence of Alexafluor488-streptavidin (AF488-SA) for 1 h. FRET between TBD and AF488-SA was measured, followed by disruption with Triton-X100 to determine the FRET for complete leakage. A. Experiments at pH 7, where the pHD peptide pHD108 is inactive. B. Experiments at pH 5, where pHD108 is active.

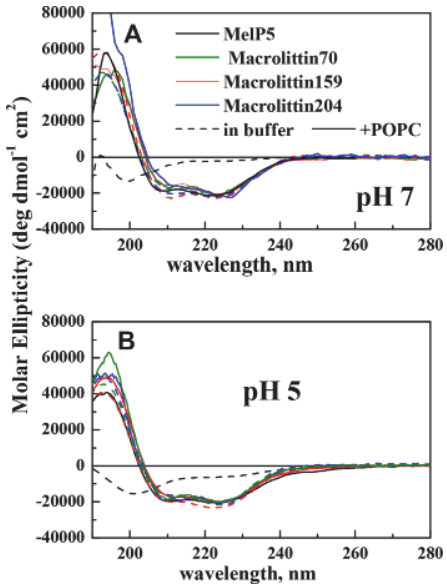

Figure 3. Solution circular dichroism spectra of macrolittins and MelP5 at 25 μM. Measurements were made before addition (dashed lines) and after addition (solid lines) of 1 mM POPC vesicles. A. Measurements made at pH 7. B. Measurements made at pH 5.

POPC to a 40 kDa dextran as a function of peptide concentration. The leakage activity curves at pH 7 are shown in Figure 2A. Macrolittins release TAMRA-biotin dextran (40 kDa) with a leakage inducing concentration of 50% effect (LIC_{50}) of P:L $\leq$ 1:800. This is remarkably potent activity for macromolecule release, matched only by the pHD peptides at pH 5 (Figure 2B). While MelP5 releases a 10 kDa dextran at similar LIC_{50},[19] its ability to release a 40 kDa is much lower, with LIC_{50} at P:L = 1:50 (Figure 2A). For comparison, the most active pHD peptides, at pH 5, release 40 kDa dextran with LIC_{50} values of P:L = 1:800,[11] similar to the macrolittins at pH 7.

We also measured macrolittin-induced dextran leakage at pH 5 (Figure 2B) to directly compare the macrolittins to the pHD peptides under identical conditions. Surprisingly, the two families have *opposite* pH dependences. Unlike the pHD peptides which gain activity at pH 5, the macrolittins are somewhat less potent at pH 5 than they are at pH 7, with LIC_{50} values between 1:150 and 1:400. However, even at pH 5, the macrolittins are more potent than MelP5. The activity of MelP5 is similar at both pH values as reported previously.[11]

Circular Dichroism and Tryptophan Fluorescence. To assess the secondary structure of the macrolittins, we measured their circular dichroism spectra, at pH 7 and pH 5, in buffer with and without lipid vesicles. The control peptide MelP5 is random coil in buffer and becomes highly helical only upon membrane binding (Figure 3). Surprisingly, the macrolittins are highly helical in buffer at pH 7 (Figure 3A), and also at pH 5 (Figure 3B), even in the absence of lipid vesicles. This unexpected finding suggests that they readily self-assemble into stable helical multimers in buffer perhaps like the melittin tetramers that form under some conditions.[23] In the presence of POPC vesicles, the macrolittins retain their well-organized α-helical secondary structure, while the control peptide MelP5 shows a sharp transition to α-helix only upon binding to vesicles.

We used the fluorescence of the single tryptophan at position 19 of the peptides to further assess their structure in buffer and in membranes. The tryptophan in MelP5, which is random coil and monomeric in buffer, has an emission maximum of 349 nm at both pH 7 and pH 5 as expected for a water-exposed tryptophan in a monomeric peptide (Figure 4). However, the macrolittins in buffer have tryptophan emission maxima from 319 to 333 nm, significantly blue-shifted from those expected for water-exposed tryptophan. This observation is consistent with our conclusion that the macrolittins form helical multimers in buffer, as multimer formation would bury the Trp residue in a less polar environment. In the presence of POPC vesicles, MelP5 and the macrolittins have very similar tryptophan emission maxima of 320−330 nm, signifying a similar environment in the membrane. These emission maxima are in the expected range for a tryptophan that is membrane inserted[24] as we have reported for MelP5[14] and the pHD peptides at pH 5 in bilayers.[11]

Oriented Circular Dichroism Spectroscopy. To determine the orientation of the macrolittin helices in bilayers, we used macrolittin159 as a representative of the family, and subjected it to oriented circular dichroism (OCD). Samples for OCD were hydrated stacked multilayers containing 5 mol % peptide. The experimental OCD spectra are shown in Figure 5, and can be compared to the theoretical OCD spectra shown as a function of fraction of peptide inserted in a membrane spanning orientation.[25] Comparison of the positions and ratios of the experimental macrolittin159 OCD spectral peaks to the theoretical peaks suggested that macrolittin159 is a membrane-spanning helix at pH 7. We estimate an inserted fraction of at least 80%. Previously, we showed that MelP5 is also a membrane-spanning helix under these conditions.[14]

Atomic Force Microscopy. We sought to directly observe the consequences of macrolittin-bilayer interactions via AFM

DOI: 10.1021/jacs.8b03026
J. Am. Chem. Soc. 2018, 140, 6441−6447

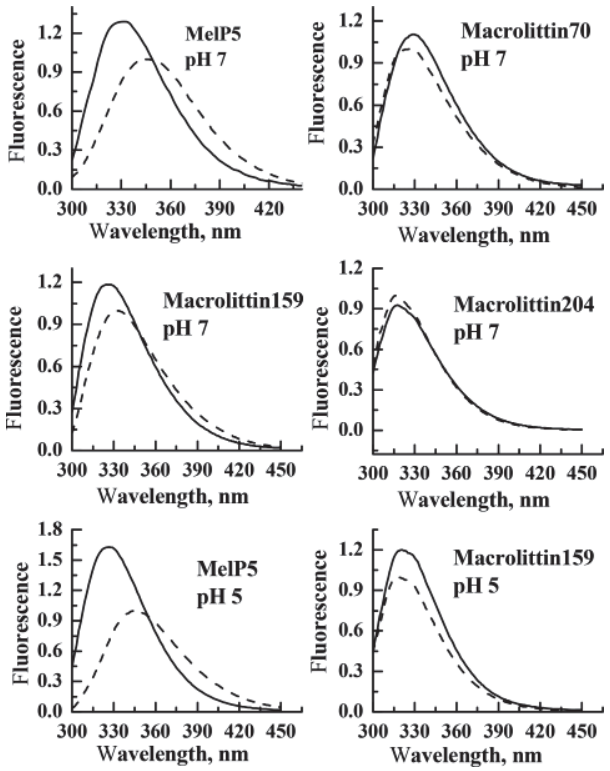

Figure 4. Tryptophan fluorescence spectra of the macrolittins and MelP5. Spectra were measured for 5 μM peptide before addition (dashed lines) and after addition (solid lines) of 1 mM POPC vesicles. Excitation was at 280 nm. Emission spectra are normalized to the maximum intensity in buffer.

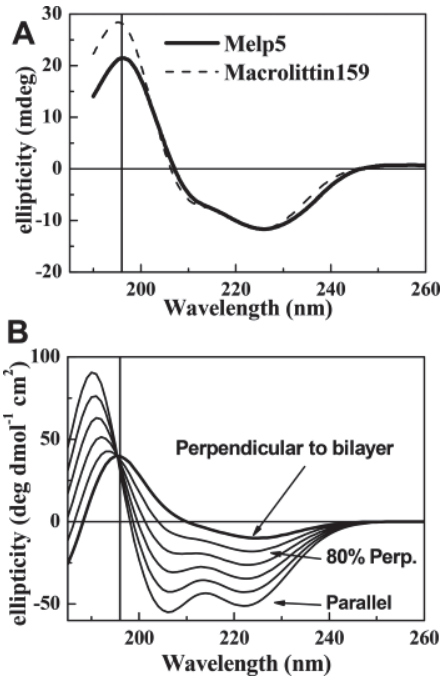

Figure 5. Oriented Circular Dichroism. A. OCD spectra are shown for macrolittin159 and for MelP5 in comparison in stacked, oriented POPC multibilayers on a quartz substrate hydrated with water through the vapor phase. Shown are the average of eight individual spectra collected at rotations around the beam axis. The lipid only spectra have been subtracted. B. Basis theoretical OCD spectra, (top and bottom curve) and linear combinations for parallel and perpendicular helices calculated as described previously.[25] The four intermediate curves are for increments of % perpendicular helix increasing by 20% per step.

imaging in physiologically relevant conditions: in fluid phase bilayers in aqueous solution at room temperature. We used macrolittin70 and compared the results to the membrane remodeling induced by MelP5. Prior to deposition onto freshly cleaved mica, vesicles of POPC were incubated with macrolittin70 at a starting P:L of 1:124. To remove loosely bound material, the samples were washed thoroughly with buffer before imaging. Nominally identical experiments using MelP5 were performed at the same P:L, and the effects of the two peptides on the bilayers was observed (Figure 6A & B). The two peptides remodeled the bilayer in different ways. The macrolittin70-treated bilayer exhibited large and deep voids as well as numerous shallow defects. Some of these voids were deep and localized, suggestive of pores across the bilayer. MelP5-treated bilayers exhibited a single shallow defect mode. In order to delineate the effects of the two peptides further, a flood mask was used to isolate only the peptide affected areas of the bilayer (affected areas were defined as bilayer defects measuring at least 0.3 nm deep, Figure 6C: inset). Histograms of defect depths were calculated for the affected areas (Figure 6C). For macrolittin70, the histogram exhibited multiple subpopulations across a broad range of defect depths, whereas MelP5 affected the bilayer in one prominent way producing voids with depths roughly 0.6 nm below the top surface. We note that the upper surface in the AFM images may represent the unmodified upper leaflet of the bilayer; however, it is difficult to rule out the alternative possibility that the top surface could represent a peptide-distorted lipid layer. Regardless of the interpretation of the top surface, it is clear that macrolittin70 and MelP5 remodeled the lipid bilayer in different ways. Under essentially the same conditions, macrolittin70 had a more multifaceted and destructive effect on the lipid bilayer structure as compared to MelP5, consistent with the more potent membrane permeabilization activity described above.

DISCUSSION

Here we describe the macrolittins, a family of peptides that release macromolecules from lipid bilayers made from zwitterionic PC lipids at very low peptide concentration and at neutral pH. Macrolittins readily enable the passage of a 40 000 Da dextran, a macromolecule with 4.5 nm hydrodynamic radius through lipid bilayers. Macromolecule release from liposomes is measurable at P:L as low as 1:5000 (20 peptides per vesicle) and reaches 50% at P:L as low as 1:1000, or 100 peptides per vesicle. Except for the pHD peptides at low pH (Figure 2B), such potent macromolecular poration by peptides in PC bilayers is unprecedented in the literature.

In the MelP5-based library from which both the macrolittins and the pHD peptides were selected, six positions had the possibility of containing an acidic aspartate or glutamate residue, or the native residue or, in some cases, another nonpolar residue (Figure 1). The selected macrolittins share a common, variable motif, always with three acidic amino acids per peptide, compared to five or six in all pHD peptides. In Figure 1D, we show the helical wheels of MelP5, the library, representative macrolittins, and representative pHD peptides. We note that these helical wheels may not be precisely correct

DOI: 10.1021/jacs.8b03026
J. Am. Chem. Soc. 2018, 140, 6441−6447

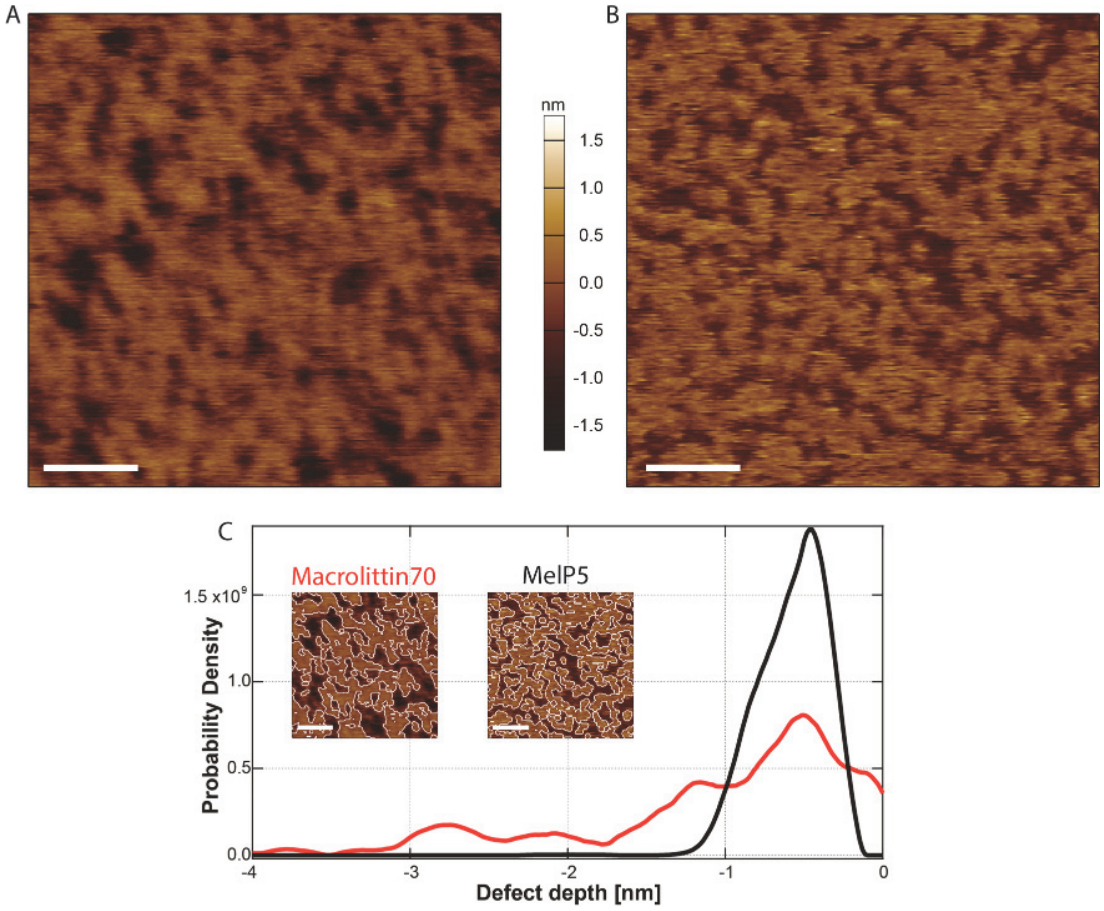

Figure 6. Membrane topography via atomic force microscopy. A. Representative AFM image of a POPC bilayer incubated with macrolittin70. B. For comparison, we show the effect of MelP5 under nominally identical conditions. C. Histograms of bilayer defect depths for both peptides (macrolittin70 in red, number of defects, N = 378; MelP5 in black, N = 1136). Inset: Images with white contours outlining defect areas. For all images, scale bars (white) are 50 nm.

because the Gly-Leu-Pro segment at residues 12−14 may be poorly structured and may lead to N- and C-terminal helices that are somewhat independent of each other. Nonetheless, the helical wheels show that the library template sequence of MelP5 is highly amphipathic with a narrow polar face width. The library contains protonatable residues spread across a face that is much wider than the polar face of MelP5 and could potentially increase the polar face angle to almost 180°. The macrolittins show a narrower polar face with acidic residues mostly in positions 4,8 and 11 or 15, which comprise the center or the acidic face. Residues 12 and 18, which are the outside-most two residues on the acidic face, are rarely found to be acidic in the macrolittins (1/10), while they are acidic most of the time (17/20) in the pHD peptides.

The fact that two acidic residues at positions 4 and 8 are nearly 100% conserved in the five macrolittins (and also in the ten pHD peptides) may indicate that they are critical for the membrane-disrupting function that we observe for both families of peptides. The core of the polar face may be important for the interactions that enable macromolecular poration. If so, the outermost residues of the wide polar face of the pHD peptides may be important for pH sensitivity. The conserved anionic residues at positions 4 and 8 are found on the same face of the N-terminal half of the helix. They are at about a 90° angle on the helical wheel from either of the two positive residues, residues 7 and 21. The fact that we found lysine over histidine in these positions in 9/10 chances indicates that having a positive charge at pH 7 is important for macrolittin function. We speculate that parallel macrolittin helices have lateral electrostatic interactions between the conserved acidic groups and the basic amino acid at position 7. Such a stabilized structure would create an amphipathic surface that could participate in a large pore. Antiparallel helices that are electrostatically stabilized by interactions between the N-terminal acidic residues and the basic residue at position 21 are also possible, however the surface formed would be less amphipathic and thus seems less likely.

The ability to fold into an amphipathic α-helix in membranes is a common property for all of the generations of peptides discussed here, and for many other membrane permeabilizing peptides.[26] The original natural parent peptide, melittin, forms an amphipathic helix in membranes that lies mostly parallel to the membrane surface and creates transient pores at moderate concentrations.[8−10,27] The synthetically evolved daughter sequence MelP5 has a more ideally amphipathic structure than melittin. It exists in a stable transmembrane configuration in PC bilayers and forms equilibrium pores[14] that release macromolecules.[19] This behavior is consistent with the observation reported here that the macrolittins also have a transmembrane orientation. Transmembrane orientation is likely a critical structural requirement for macromolecular poration.[14]

DOI: 10.1021/jacs.8b03026
J. Am. Chem. Soc. 2018, 140, 6441−6447

We do not yet know the pore structure, but we can narrow the possibilities by considering minimal possible geometries. An extruded unilamellar vesicle is nominally 50 nm in radius, has about 100 000 lipids and has a surface area of $\sim 3 \times 10^4$ nm^2. A dextran of 40 kDa has a hydrodynamic radius of ~4.5 nm meaning that a "pore" of at least 80 nm^2 (5 nm radius, 1/300 of the vesicle surface area) would be minimally required to pass it. Pores of this size are consistent with the AFM images presented in Figure 6. If we consider a classical barrel-stave pore, in which the peptides are laterally close-packed, then the pore would have a circumference of at least 30 nm, which would require ≥30 peptides to line it. Thus, a lipid vesicle can have only a few pores at P:L ~ 1:1000 (100 peptides per vesicle), where activity is high.

With such large pathways across the bilayer, it may be more fruitful to consider a structural model in which these amphipathic peptides drive bilayer thinning and stabilize exposed bilayer edges by reducing line tension at low concentration as other amphipathic peptides, proteins, polymers, and detergents do at higher concentration.[28−31] The AFM results are consistent with the macrolittins having a dramatic effect on bilayer thickness and structure. In this scenario, individual peptides are not in direct contact with each other, but instead cooperatively alter lipid thickness and curvature to stabilize an exposed bilayer edge in a so-called toroidal pore geometry.[32−34] In this architecture, electrostatic stabilization remains possible because such interactions have a long-range. Fewer peptides could be needed to stabilize such a toroidal "pore". The critical interactions, in this case, would be curvature-dependent interactions between peptides and the bilayers that may work synergistically with electrostatic interactions between peptides.

AUTHOR INFORMATION

Corresponding Authors

*wwimley@tulane.edu

*kh@jhu.edu

ORCID

Gavin M. King: 0000-0002-5811-7012

William C. Wimley: 0000-0003-2967-5186

Notes

The authors declare no competing financial interest.

ACKNOWLEDGMENTS

We wish to acknowledge Krishna Sigdel for assistance with lipid quantification. Funded by NIH R01 GM111824 and NSF DMR 1710053 (WCW), NSF DMR 1709892 (KH), and NSF DMR 1709792 (GMK).

REFERENCES

(1) Wang, Z.; Wang, G. *Nucleic Acids Res.* **2004**, *32*, 590D−592.

(2) Hancock, R. E.; Sahl, H. G. *Nat. Biotechnol.* **2006**, *24*, 1551−1557.

(3) Pan, H.; Soman, N. R.; Schlesinger, P. H.; Lanza, G. M.; Wickline, S. A. *Rev. Nanomed. Nanobiotechnol* **2011**, *3*, 318−327.

(4) Hood, J. L.; Jallouk, A. P.; Campbell, N.; Ratner, L.; Wickline, S. A. *Antiviral Ther.* **2012**, *18*, 95−103.

(5) Gerlach, S. L.; Rathinakumar, R.; Chakravarty, G.; Goransson, U.; Wimley, W. C.; Darwin, S. P.; Mondal, D. *Biopolymers* **2010**, *94*, 617−625.

(6) Suhorutsenko, J.; Oskolkov, N.; Arukuusk, P.; Kurrikoff, K.; Eriste, E.; Copolovici, D. M.; Langel, U. *Bioconjugate Chem.* **2011**, *22*, 2255−2262.

(7) Bukovnik, U.; Gao, J.; Cook, G. A.; Shank, L. P.; Seabra, M. B.; Schultz, B. D.; Iwamoto, T.; Chen, J.; Tomich, J. M. *Biochim. Biophys. Acta, Biomembr.* **2012**, *1818*, 1039−1048.

(8) Krauson, A. J.; He, J.; Wimley, W. C. *Biochim. Biophys. Acta, Biomembr.* **2012**, *1818*, 1625−1632.

(9) Wiedman, G.; Herman, K.; Searson, P.; Wimley, W. C.; Hristova, K. *Biochim. Biophys. Acta, Biomembr.* **2013**, *1828*, 1357−1364.

(10) Wimley, W. C. *Biophys. J.* **2018**, *114*, 251−253.

(11) Wiedman, G.; Kim, S. Y.; Zapata-Mercado, E.; Wimley, W. C.; Hristova, K. *J. Am. Chem. Soc.* **2017**, *139*, 937−945.

(12) Krauson, A. J.; Hall, O. M.; Fuselier, T.; Starr, C. G.; Kauffman, W. B.; Wimley, W. C. *J. Am. Chem. Soc.* **2015**, *137*, 16144−16152.

(13) Krauson, A. J.; He, J.; Hoffmann, A. R.; Wimley, A. W.; Wimley, W. C. *ACS Chem. Biol.* **2013**, *8*, 823−831.

(14) Krauson, A. J.; He, J.; Wimley, W. C. *J. Am. Chem. Soc.* **2012**, *134*, 12732−12741.

(15) Marks, J. R.; Placone, J.; Hristova, K.; Wimley, W. C. *J. Am. Chem. Soc.* **2011**, *133*, 8995−9004.

(16) Rathinakumar, R.; Wimley, W. C. *FASEB J.* **2010**, *24*, 3232−3238.

(17) Rathinakumar, R.; Wimley, W. C. *J. Am. Chem. Soc.* **2008**, *130*, 9849−9858.

(18) Rausch, J. M.; Marks, J. R.; Wimley, W. C. *Proc. Natl. Acad. Sci. U. S. A.* **2005**, *102*, 10511−10515.

(19) Wiedman, G.; Fuselier, T.; He, J.; Searson, P. C.; Hristova, K.; Wimley, W. C. *J. Am. Chem. Soc.* **2014**, *136*, 4724−4731.

(20) Stewart, J. C. *Anal. Biochem.* **1980**, *104*, 10−14.

(21) Wimley, W. C.; Selsted, M. E.; White, S. H. *Protein Sci.* **1994**, *3*, 1362−1373.

(22) Sanganna Gari, R. R.; Frey, N. C.; Mao, L.; Randall, L.; King, G. M. *J. Biol. Chem.* **2013**, *288*, 16848−16854.

(23) Terwilliger, T. C.; Weissman, L.; Eisenberg, D. *Biophys. J.* **1982**, *37*, 353−361.

(24) Ladokhin, A. S.; Jayasinghe, S.; White, S. H. *Anal. Biochem.* **2000**, *285*, 235−245.

(25) Wu, Y.; Huang, H. W.; Olah, G. A. *Biophys. J.* **1990**, *57*, 797−806.

(26) Bechinger, B. *J. Membr. Biol.* **1997**, *156*, 197−211.

(27) Frey, S.; Tamm, L. K. *Biophys. J.* **1991**, *60*, 922−930.

(28) Vargas, C.; Arenas, R. C.; Frotscher, E.; Keller, S. *Nanoscale* **2015**, *7*, 20685−20696.

(29) Epand, R. M.; Shai, Y.; Segrest, J. P.; Anantharamiah, G. M. *Biopolymers* **1995**, *37*, 319−338.

(30) De Angelis, A. A.; Opella, S. J. *Nat. Protoc.* **2007**, *2*, 2332−2338.

(31) Gazzara, J. A.; Phillips, M. C.; Lund-Katz, S.; Palgunachari, M. C.; Segrest, J. P.; Anantharamaiah, G. M.; Snow, J. W. *J. Lipid Res.* **1997**, *38*, 2134−2146.

(32) Sengupta, D.; Leontiadou, H.; Mark, A. E.; Marrink, S. J. *Biochim. Biophys. Acta, Biomembr.* **2008**, *1778*, 2308−2317.

(33) Allende, D.; Simon, S. A.; McIntosh, T. J. *Biophys. J.* **2005**, *88*, 1828−1837.

(34) Yang, L.; Harroun, T. A.; Weiss, T. M.; Ding, L.; Huang, H. W. *Biophys. J.* **2001**, *81*, 1475−1485.

DOI: 10.1021/jacs.8b03026
J. Am. Chem. Soc. 2018, 140, 6441−6447